


## AUTHOR QUERY FORM

 <b>ELSEVIER</b>	<b>Journal: ATMOS</b>  <b>Article Number: 2990</b>	<b>Please e-mail or fax your responses and any corrections to:</b> <b>Nambiar, Aparna</b> <b>E-mail: <a href="mailto:Corrections.ESCH@elsevier.spitech.com">Corrections.ESCH@elsevier.spitech.com</a></b> <b>Fax: +1 619 699 6721</b>
--	--	--

Dear Author,

Please check your proof carefully and mark all corrections at the appropriate place in the proof (e.g., by using on-screen annotation in the PDF file) or compile them in a separate list. Note: if you opt to annotate the file with software other than Adobe Reader then please also highlight the appropriate place in the PDF file. To ensure fast publication of your paper please return your corrections within 48 hours.

For correction or revision of any artwork, please consult <http://www.elsevier.com/artworkinstructions>.

Any queries or remarks that have arisen during the processing of your manuscript are listed below and highlighted by flags in the proof. Click on the 'Q' link to go to the location in the proof.

<b>Location in article</b>	<b>Query / Remark: <a href="#">click on the Q link to go</a> Please insert your reply or correction at the corresponding line in the proof</b>
<a href="#">Q1, Q37</a>	Please confirm that given names and surnames have been identified correctly.
<a href="#">Q2</a>	Please provide a definition for the significance of superscripted "1" in the table.
<a href="#">Q3</a>	Please check footnote here if it is appropriate, and correct if necessary.
<a href="#">Q4</a>	Please check the presentation of Table 4, and correct if necessary.
<a href="#">Q5</a>	The country name "The Netherlands" has been inserted for the last affiliation. Please check, and correct if necessary.
<a href="#">Q6</a>	Please identify the name of the corresponding author and provide the correspondence details.
<a href="#">Q7</a>	Highlights should consist of only 125 characters per bullet point, including spaces. However, the Highlights provided for this item exceed the maximum requirement; thus, they were not captured. Kindly provide replacement Highlights that conform to the requirement for us to proceed. For more information, please see the Guide for Authors.
<a href="#">Q8, Q11, Q13, Q15, Q19, Q21, Q27, Q29, Q30, Q32</a>	This sentence has been slightly modified for clarity. Please check that the meaning is still correct, and amend if necessary.
<a href="#">Q9</a>	The citation "Watkins and Kolokotroni, 2012" has been changed to match the author name/date in the reference list. Please check here and in subsequent occurrences, and correct if necessary.
<a href="#">Q10</a>	The citation "Takahashi (2008)" has been changed to match the author name/date in the reference list. Please check here and in subsequent occurrences, and correct if necessary.
<a href="#">Q12</a>	The citation "Solomon et al., 2007" has been changed to match the author name/date in the reference list. Please check here and in subsequent occurrences, and correct if necessary.
<a href="#">Q14</a>	The citation "Skamarock et al. 2007" has been changed to match the author name/date in the reference list. Please check here and in subsequent occurrences, and correct if necessary.
<a href="#">Q16, Q22</a>	The citation "Skamarock et al. (2007)" has been changed to match the author name/date in the reference list. Please check here and in subsequent occurrences, and correct if necessary.

<a href="#">Q17</a>	The citation “Skamarock et al., 2007” has been changed to match the author name/date in the reference list. Please check here and in subsequent occurrences, and correct if necessary.
<a href="#">Q18</a>	The citation “Mitchell, 2005” has been changed to match the author name/date in the reference list. Please check here and in subsequent occurrences, and correct if necessary.
<a href="#">Q20, Q28</a>	A closing parenthesis was placed here. Please check, and correct if necessary.
<a href="#">Q23</a>	The citation “NCAR et al., 2002” has been changed to match the author name/date in the reference list. Please check here and in subsequent occurrences, and correct if necessary.
<a href="#">Q24</a>	Citation “Pathirana, et al. 2003” has not been found in the reference list. Please supply full details for this reference.
<a href="#">Q25</a>	Citation “Lih and Yeh, 2008” has not been found in the reference list. Please supply full details for this reference.
<a href="#">Q26</a>	Citation “Yang et al., 2008” has not been found in the reference list. Please supply full details for this reference.
<a href="#">Q31</a>	Citation “Meir, 2013” has not been found in the reference list. Please supply full details for this reference.
<a href="#">Q33</a>	Uncited reference: This section comprises references that occur in the reference list but not in the body of the text. Please position each reference in the text or, alternatively, delete it. Thank you.
<a href="#">Q34, Q35, Q36</a>	Supplementary caption was not provided. Please check suggested data if appropriate and correct if necessary.
<a href="#">Q38</a>	Please provide the volume number and page range for the bibliography in ‘Kelkar, 2005’.
<a href="#">Q39</a>	Please provide the volume number and page range for the bibliography in ‘Meir et al., 2013’.
<a href="#">Q40</a>	<p>Please confirm that surnames have been identified correctly.</p> <div style="border: 1px solid black; padding: 5px; width: fit-content; margin-left: auto; margin-right: auto;"> <p>Please check this box if you have no corrections to make to the PDF file. <input type="checkbox"/></p> </div>

Thank you for your assistance.

Q34 Supplementary material 1.

Q35 Video 1.

Q36 Video 2.



ELSEVIER

Contents lists available at ScienceDirect

## Atmospheric Research

journal homepage: [www.elsevier.com/locate/atmos](http://www.elsevier.com/locate/atmos)

## Q7 Impact of urban growth-driven landuse change on 2 microclimate and extreme precipitation – A sensitivity study

Q1 Q6 Assela Pathirana<sup>a</sup>, Hailu B. Deneke<sup>a</sup>, William Veerbeek<sup>b</sup>,  
4 Chris Zevenbergen<sup>a,b,c</sup>, Allan T. Banda<sup>a</sup>

5 <sup>a</sup> UNESCO-IHE Institute for Water Education, Westvest 7, Delft 2611AX, The Netherlands

6 <sup>b</sup> Department of Hydraulic Engineering, Faculty of Civil Engineering and Geosciences, Delft University of Technology, Stevinweg 1, Delft 2628CN, The Netherlands

Q5 <sup>c</sup> Dura Vermeer Groep NV, Orfeeschouw 30, 2726JE Zoetermeer, The Netherlands

8

### 10 A R T I C L E I N F O

#### 12 Article history:

13 Received 9 March 2012

14 Received in revised form 3 October 2013

15 Accepted 6 October 2013

16 Available online xxxx

#### 39 Keywords:

40 Urbanisation

41 Urban heat island

42 Urban growth

43 Landuse change

44 Atmospheric model

45 Hydrometeorology

### A B S T R A C T

More than half of the humanity lives in cities and many cities are growing in size at a phenomenal 17  
rate. Urbanisation-driven landuse change influences the local hydrometeorological processes, 18  
changes the urban micro-climate and sometimes affects the precipitation significantly. Under- 19  
standing the feedback of urbanisation driven micro-climatic changes on the rainfall process is a 20  
timely challenge. In this study we attempt to investigate the impact of urban growth driven 21  
landuse change on the changes in the extreme rainfall in and around cities, by means of sensitivity 22  
studies. We conduct three sets of controlled numerical experiments using a mesoscale atmo- 23  
spheric model coupled with a landuse model to investigate the hypothesis that the increasing 24  
urbanisation causes a significant increase of extreme rainfall values. First we conduct an ensemble 25 Q8  
of purely idealised simulations where we show that there is a significant increase of high intensity 26  
rainfall with the increase of urban landuse. Then four selected extreme rainfall events of different 27  
tropical cities were simulated with first current level of urbanisation and then (ideally) expanded 28  
urban areas. Three out of the four cases show a significant increase of local extreme rainfall when 29  
the urban area is increased. Finally, we conducted a focused study on the city of Mumbai, India: A 30  
landscape dynamics model Dinamica-EGO was used to develop a future urban growth scenario 31  
based on past trends. The predicted future landuse changes, with current landuse as control, were 32  
used as an input to the atmospheric model. The model was integrated for four historical cases 33  
which showed that, had these events occurred with the future landuse, the extreme rainfall 34  
outcome would have been significantly more severe. An analysis of extreme rainfall showed 35  
that hourly 10-year and 50-year rainfall would increase in frequency to 3-year and 22-year 36  
respectively. 37

© 2013 Elsevier B.V. All rights reserved. 38

### 49 1. Introduction

50 Today, more than half of the world's population lives in 51  
cities. Due to the increasing concentration of businesses 52  
and infrastructure, the urbanisation process continues at 53  
a phenomenal rate. The urban water cycle and the local 54  
climatic environment are invariably affected by the urban 55  
growth (Foley et al., 2005). The causal relationship between

urbanisation and increased stormwater flows due to the 56  
hydrological changes on the surface is well understood and 57  
quantified. It is common knowledge that the urbanisation 58  
increases runoff due to the retardation of infiltration and 59  
evapotranspiration processes, and decreases the resistance to 60  
flow. The question whether the rainfall itself is changed due 61  
to the micro-climatic changes above cities as a consequence of 62  
urban landuse change, was being asked since the 1960s. Today, 63  
there is an increasing body of evidence that the changes in 64  
the radiation and heat balance affected by changes in surface 65  
albedo and vegetation cover on the urban micro-climate 66

E-mail address: [assela@pathirana.net](mailto:assela@pathirana.net) (A. Pathirana).

0169-8095/\$ – see front matter © 2013 Elsevier B.V. All rights reserved.  
<http://dx.doi.org/10.1016/j.atmosres.2013.10.005>

Please cite this article as: Pathirana, A., et al., Impact of urban growth-driven landuse change on microclimate and extreme precipitation – A sensitivity study, Atmos. Res. (2013), <http://dx.doi.org/10.1016/j.atmosres.2013.10.005>

67 can have significant impacts on the precipitation patterns  
 Q9 over urban centres and their surroundings (Watkins and  
 69 Kolokotroni, 2013). These hydro-meteorological effects are  
 70 caused by a) microphysical changes resulting from urban  
 71 pollution, b) increased surface roughness due to urban  
 72 structures and c) heat anomalies resulting from changes in  
 73 albedo and latent heat flux – ‘urban heat island (UHI)’  
 74 (Sagan et al., 1979). While the urban heat island effect  
 75 on radiation, temperature and wind has been documented  
 76 relatively early (Taha et al. (1988), Landsberg (1981) and  
 77 references therein) modelling investigations on the impact  
 78 on rainfall appeared late in the literature. Some of the  
 79 difficulties in the latter endeavour is summarised by Lowry  
 80 (1998). There have been many empirical investigations  
 81 indicating the possibility of the urban growth and the  
 82 resulting UHI modulating precipitation (e.g. Shepherd,  
 83 2006; Jauregui, 1996; Subbiah et al., 1990; Lin et al.,  
 Q10 2008, 2009; Takahashi, 2003). Of particular interest is the  
 85 Metropolitan Meteorological Experiment (METROMEX), a  
 86 major observational study conducted in the US in the  
 87 1970s (Changnon, 1979). METROMEX findings showed that  
 88 precipitation down-wind of large cities can increase 5%–  
 89 25% from background values (Shepherd, 2005). Charabi  
 90 and Bakhit (2011) used meteorological data measured over  
 91 a period of one year over the city of Muscat, Oman, to  
 92 study the urban heat island over the city. They found that  
 93 the hottest locations occur at the compactly built ‘old  
 94 Muscat’ neighbourhoods in narrow valleys. During the rare  
 95 winter rainfall spells the intensity of UHI decreased. Meir  
 96 et al. (2013) examined two 2011 heat events in New York  
 97 City to evaluate the predictive ability of 1 km resolution US  
 98 Navy’s Coupled Ocean/Atmosphere Mesoscale Prediction  
 99 System (COAMPS) model and 12 km resolution North  
 100 American Mesoscale (NAM) implementation of WRF model  
 101 using a land and coastline based observation networks. The  
 102 high resolution model was able to capture the key features of  
 103 the heat events, where urban rural temperature differences  
 104 were as high as 4–5 °C.

105 Numerical modelling experiments are extremely relevant  
 106 in understanding and quantifying the possible effect of UHI on  
 107 rainfall, as this is probably the only way to conduct controlled  
 108 studies at city and regional scales to investigate the sensitivity  
 109 of various influencing parameters. Shepherd (2005) noted that  
 110 there had been relatively few studies in this field. Since then  
 111 there have been a number of reports on such experiments.  
 112 Shem and Shepherd (2009) conducted controlled experiments  
 113 on three landuse scenarios for Atlanta, USA, with different  
 114 levels of urbanisation and concluded that there is a significant  
 115 impact of UHI on cumulative rainfall quantities resulting in  
 116 increases of 10% to 13% for increased urbanisation. Lin et al.  
 117 (2008) reported results of numerical experiments comparing  
 118 impacts of UHI on rainfall by comparing the atmospheric  
 119 response to synthetically increasing urban area in the case  
 120 of Taiwan. They concluded that the UHI interaction with  
 121 summer-time sea-breeze and mountain uplifting contributes  
 122 significantly to increase rainfall in the mountainous areas on  
 123 the leeward side of the city. On the other hand, analysing the  
 124 7th July 2004 thunderstorm over Baltimore, USA by means of  
 125 controlled modelling studies, Ntelekos et al. (2008) concluded  
 126 that UHI did not contribute to the heavy rainfall during the  
 127 event.

128 Most of the studies in the recent literature on the UHI and  
 129 precipitation had a strong focus on mesoscale meteorology,  
 130 and often stopped short of making impact assessment at  
 131 the urban scale. It is indeed challenging to translate the  
 132 predictions of the impacts of UHI driven changes in the  
 133 meteorological events to forms that can be readily used by  
 134 civil engineers to plan urban water infrastructure. Such an  
 135 attempt would invariably result in large uncertainties and  
 136 could leave many gaps in reasoning that future research  
 137 has to fill in. However, the possible strong causal link of  
 138 urbanisation on urban extreme rainfall can no longer be  
 139 ignored, particularly in the context of rapid urban growth  
 140 and numerous external pressures like global climate change.  
 141 There is a growing interest on the role of land cover and  
 142 landuse change on climate change (Solomon et al., 2005),  
 Q11 Q12 partially due to the awareness raised by events like the  
 143 Nerima heavy rainfall (Kawabata et al., 2007) and general  
 144 indications of significant increase of extreme rainfall in  
 145 rapidly urbanising locations like the Indian subcontinent  
 146 that are suspected to be triggered by UHI (Kishtawal et al.,  
 147 2010). However, in order to understand the impacts on the  
 148 issue of urban drainage and flooding, it is important to  
 149 understand the influence of UHI on short-term, extreme  
 150 rainfall – the driving force on urban storm water system. The  
 151 fact that most populous cities, which happen to be in the  
 152 Third World, have already over-stressed that storm drainage  
 Q13 systems further increase the relevance of it. 154

155 In this paper, we present the results of a series of numerical  
 156 experiments conducted using a state of the art, 3D mesoscale  
 atmospheric model – WRF-ARW (Skamarock et al., 2005) – in  
 Q14 order to attempt to understand the impact of urbanisation-  
 158 driven landuse change on the extreme rainfall events in and  
 159 around cities. Our hypothesis is that changes in urban landuse  
 160 cause significant changes in extreme rainfall in urban centres  
 161 and surrounding areas. We propose that these changes will  
 162 have significant implications on the planning and imple-  
 163 mentation of urban drainage projects, mitigation of urban  
 164 floods and ensuring the human security in cities in general.  
 165 It should be noted that we limit the scope of this sensitivity  
 166 study to the possible changes in the urban heat budget, due to  
 167 changes in the thermal properties (radiative, latent heat) of  
 168 urban landscape. We ignore the possible changes in boundary  
 169 layer roughness (due to tall buildings) and microphysical  
 170 changes due to urban pollution. 171

172 First we present the results of idealised experiments that  
 173 indicate the sensitivity of increase of urban land use to rainfall  
 174 and the related mechanisms. For the second set of experiments,  
 175 we have selected a number of extreme rainfall events from  
 176 around the world that caused significant urban flooding. We  
 177 conducted ‘what-if’ type of analyses on these events. We  
 178 introduced a simplified artificial urbanisation with the scenario  
 179 that the city grows to twice its original diameter and investigate  
 180 what level of influence this ‘urban-growth’ would have on the  
 181 magnitude of rainfall. Finally, for the City of Mumbai, we conduct  
 182 detailed urban growth modelling, that would give many more  
 Q15 realistic extrapolations of landuse change during the next two  
 183 decades based on historical trends and various influencing  
 184 spatial parameters. We used standard statistical techniques used  
 185 in rainfall frequency analysis to interpret the results in the  
 186 context of urban storm drainage design and urban flooding, so as  
 187 to demonstrate the practical implications of the findings. 188

189 **2. WRF-ARW model**

190 WRF-ARW model numerically solves the four con-  
 191 servation relationships, namely mass, momentum and heat  
 192 conservation of air and mass conservation including phase  
 193 changes of water, by a non-hydrostatic 3D set of equations.

The model uses terrain-following vertical coordinate system 194  
 and square grid horizontal coordinates with vector and scalar 195  
 quantities staggered on the grid. With the initial conditions 196  
 provided for the entire 3D domain and lateral boundary 197  
 conditions for the entire duration of the run, the model uses 198  
 an explicit 2nd/3rd order Runge-Kutta scheme to explicitly 199

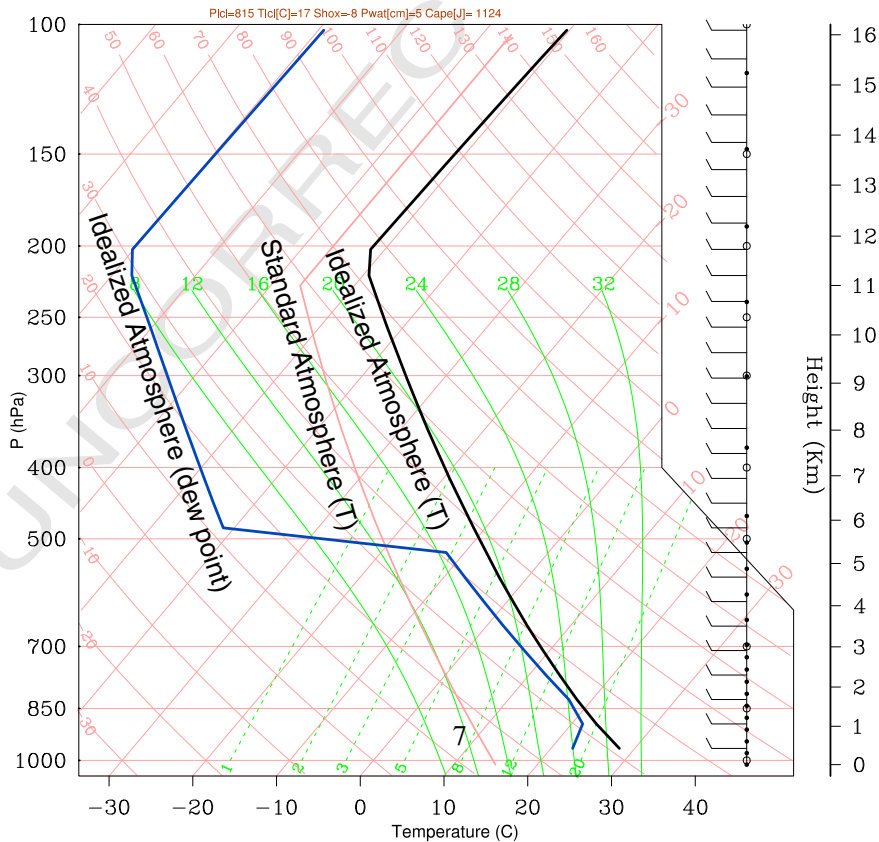
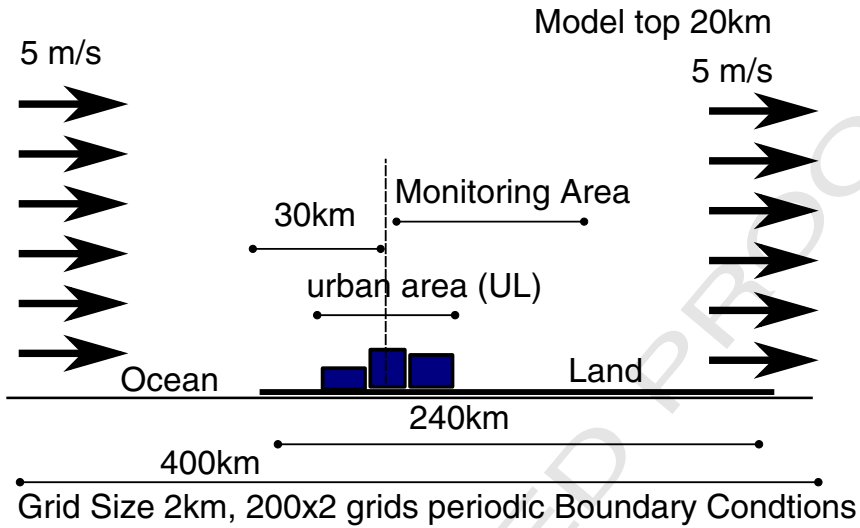


Fig. 1. The model domain for idealised experiments (top). Log-P-Skew-t plot for the atmosphere profile (bottom).



200 solve the system forward in time. The top boundary condition is parameterised often as a constant pressure surface and solar radiation is calculated based on the geographic location and cloud cover. The bottom boundary is provided by a surface scheme that could be a layered thermal diffusion model or a sophisticated landuse model that explicitly considers the vegetation and moisture effects of the surface. The planetary boundary layer is also modelled. The model physics include the full representation of the cloud microphysics that includes three phases of water and up to six classes of hydrometeors. The full description of the WRF-ARW model is given by Skamarock et al. (2005). The model is suitable for both operational use (e.g. weather forecasting) and research studies.

214 **3. Idealised model**

215 When testing a hypothesis, experimentation is arguably the most reliable approach, and the equivalent of it in large-scale environmental modelling is idealised numerical studies. Under precisely controlled conditions, repeatable numerical experiments are conducted with only a single parameter changed at a time. In the field of atmospheric science, there have been numerous applications of this technique to investigate various hypotheses (Doyle and Durran, 2001; Pathirana et al., 2005, 2007; Li, 2006). In order to test the hypothesis we stated above, we used WRF-ARW model (Skamarock et al., 2005) to simulate a 2-dimensional model domain whose essential features are illustrated in Fig. 1 (top). The domain possesses only three landuse categories: 16 – Water Bodies to represent ocean, 18 – Wooded Wetlands and 01 – Urban and Built-up Land (USGS Land Use/Land Cover System Legend). Table 1 lists important physical parameters of the three landuse types used. The model was set-up with a coupled land-surface model, Noah-LSM (Mitchell, 2000) in order to represent the vegetation and moisture effects on the surface. The lapse rate of the atmosphere in the idealised experiment was very similar in shape to that of the standard atmosphere, but the temperatures being higher values (to suit tropical conditions). The troposphere is conditionally unstable – once the surface heats up, this easily leads to convective break up. Up to about 5 km altitude the atmosphere is quite moist, in encouraging the development of rainfall. The Log P skew-T plot is shown in Fig. 1 (bottom). Idealised domains were located at [0,0] (on the equator at 0 longitude).

t1.1 **Table 1**

t1.2 Important physical parameters associated with three landuse types.

t1.3	Landuse type	Urban and built-up land	Water bodies	Wooded wetlands
t1.4	USGS index (–)	1	16	18
t1.5	Albedo (%)	15	8	14
t1.6	Soil moisture (frac.)	0.1	1	0.35
t1.7	Surface emissivity (frac.)	0.88	0.98	0.95
t1.8	Roughness length (m)	0.5	0.0001	0.4
t1.9	Leaf area index (–)	1	0.01	5.8
t1.10	Green vegetation fraction (frac.)	0.1	0	0.6
t1.11	Rooting depth (soil layer index)	1	0	2
t1.12	Stomatal resistance (s m <sup>-1</sup> )	200	100	100

250 The initial conditions were such that the entire modelling domain had a uniform 5 m/s wind field in x-direction (Fig. 1). The lateral boundary conditions were periodic in both x and y-directions. In effect this set-up recycles the wind field exiting at the end of the domain to the beginning of the domain. Since the ‘ocean’ stretch provided is inadequate to keep replenishing the water vapour, there is a limit to the total quantity of rainfall that the system will produce however long the simulation time is.

268 The model was integrated for a 12 h period with different sizes of urban area (UL from 0 (control) to 40 km, in steps of 4 km). In order to obtain a more statistically representative result, the simulations at each UL were repeated ten times with slightly different initial conditions (random perturbations of velocity, temperature and moisture). The ensemble results are shown in Fig. 2 for the ‘monitoring area’ (60 km stretch from the centre of the urban patch) shown in Fig. 1. The high intensity rainfall amount shows a statistically significant relationship with the amount of urbanisation. The same analysis for the rainfall of the entire modelling domain (as opposed to the 60 km monitoring area) did not show a statistically significant trend of rainfall with urbanisation (not shown). Furthermore, the rainfall in the region windward of the urban patch showed a statistically significant reduction of high intensity rainfall.

284 All the experiments started at 05:50 local time (05:50 GMT). The initial surface temperature was set uniformly: 287 K for ocean and 290 K for land. The model setup considers solar heating of surface (using MM5 short-wave radiation scheme). The ‘sunrise’ occurs soon after the model starts. In around 3 h the surface starts to heat up as the sun rises. The heat build-up is faster on the urban patch resulting in convective activity aloft (Fig. 3(left)). The resulting convective break-up aids in developing rainfall initially in the lee-side of the urban patch within an hour (Fig. 3 (right)).

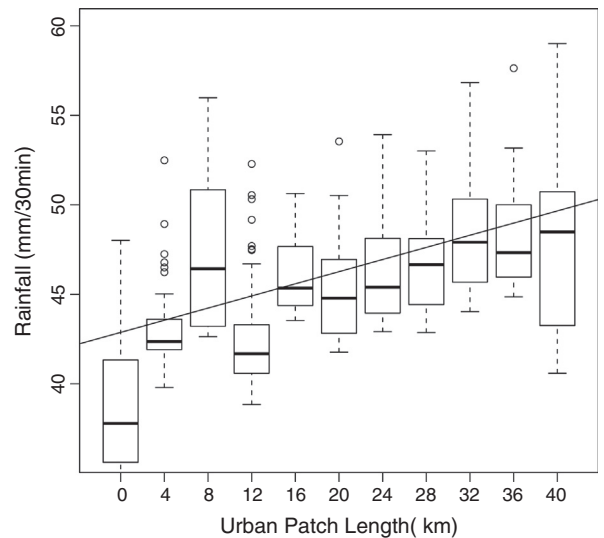


Fig. 2. The largest 25% of grid-level rainfall observed over the 60 km monitoring area. All 30 min rainfall values of each ensemble set (i.e. all simulations for a specific length of urban patch) were pooled and sorted in the order of descending intensities. Then the first 25% were used to produce the corresponding box plot.

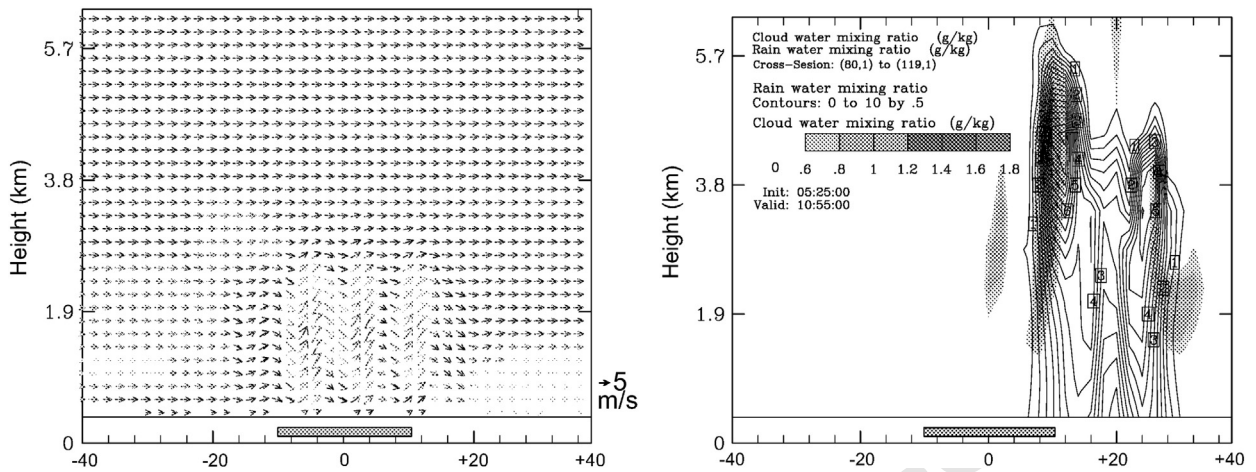


Fig. 3. Cross sections of a simulation with 20 km urban patch. Left: wind vectors at 09:55 h (with vertical exaggeration of 50) shows the initiation of convective activity aloft the urban patch (grey bar). Right: cloud formation and rainfall at 10:55 h. The precipitation starts at the lee-side of the urban-patch.

294 **4. Semi-idealised case studies**

295 For the second phase of the study, we selected four Asian  
 296 cities of varied sizes, that have had faced urban floods due to  
 Q20 local heavy precipitation during the last decade (Table 2).  
 298 The objective of the second phase was to ascertain, in the  
 299 case of historical rainstorms, whether the extreme rainfall  
 300 outcome would be significantly different, if these events  
 301 would happen in a situation where a large urban growth has  
 302 taken place. At this stage we did not attempt to realistically  
 303 model the urban growth of each city, but considered a  
 304 situation where the urban landuse has filled an area twice the  
 305 current city size ('Future scenario'). Fig. 4 shows the im-  
 Q21 plemented change for the case of the city of Colombo. In this  
 307 experiment the urban expansion introduced was not realistic  
 308 by any means. How this change was implemented in the  
 309 model is explained in the following section. The control  
 310 experiments (the 'Present scenario') were conducted using  
 311 the current landuse distribution. The initial and boundary  
 312 conditions for both sets of experiments were obtained from  
 313 actual historical atmospheric conditions during the event,  
 314 provided by NCEP-FNL Operational Global Analysis data at  
 315 1° × 1° resolution at every 6 h. In order to facilitate smooth  
 316 interpolation of this coarse-resolution, global data, we used a  
 317 three level nesting scheme shown in Fig. 5 (shown for the  
 318 case of Mumbai City). Only the innermost (5 km) grid was  
 319 subjected to further analysis. In this scenario instead of  
 320 Noah-LSM, we used the 5 layer thermal diffusion scheme  
 321 (originally developed for the MM5 model, therefore also  
 322 known as MM5-scheme), in order to save computing time.  
 Q22 This model is further explained in Skamarock et al. (2005).

4.1. Details of implementing landuse change by urbanisation 324

325 Conducting a non-idealised WRF/Noah simulation can be  
 326 divided into three steps (NCAR et al., 2000): 1. Setting up of the  
 Q23 model domain and static data. 2. Creating 3D initial and  
 327 boundary condition data and 3. Running the model. In this set  
 328 of experiments we conducted all three steps using standard  
 329 data for the 'Present scenario'. The domain files of the step 1 of  
 330 the 'Present scenario' were modified by changing only their  
 331 vegetation fraction and albedo values to obtain the 'Future  
 332 scenario'. We decreased albedo by 20% and vegetation fraction  
 333 by 75% of the average background values to indicate the  
 334 transition from non-urban to urban landuse. These values are  
 335 in agreement with past experimental and theoretical studies  
 336 (Royer et al., 1988). These changes were implemented in the  
 337 modelling as follows: WRF model's pre-processor calculates  
 338 the vegetation fraction and albedo (among other parameters)  
 339 based on landuse data, when preparing the input files for the  
 340 model. Instead of changing the input landuse maps, we directly  
 341 modified these input file to change vegetation fraction and  
 342 albedo. Then the resulting data was used to perform steps 2  
 343 and 3 for 'Future' scenario. Therefore the only difference of  
 344 'Future' scenario from the 'Present' is the decreased albedo and  
 345 vegetation fraction. 346

4.2. Model validation 347

348 Each case was first run for the 'Present' scenario and the  
 349 rainfall outcome was compared against reported events. 349  
 350 However, this was only a qualitative comparison, to check  
 351 whether the model produces a rainfall distribution that is 351

t2.1 **Table 2**  
 t2.2 Cities selected for the semi-idealised urbanisation sensitivity experiment.

t2.4 Q2	City	Country/region	Population (millions)	Area sq. km	Event type	Period <sup>1</sup>
t2.4	Colombo	Sri Lanka/South Asia	6	37	Monsoon, flood.	2–7/May/2007
t2.5	Dhaka	Bangladesh/South Asia	13	304	Monsoon, flood.	7–17/Jul/2007
t2.6	Mumbai	India/South Asia	14	438	Monsoon, flood.	1–6/Jul/2007
t2.7	Taipei	Taiwan/South-east Asia	2.6	271	Monsoon, Flood.	6–10/Oct/2008



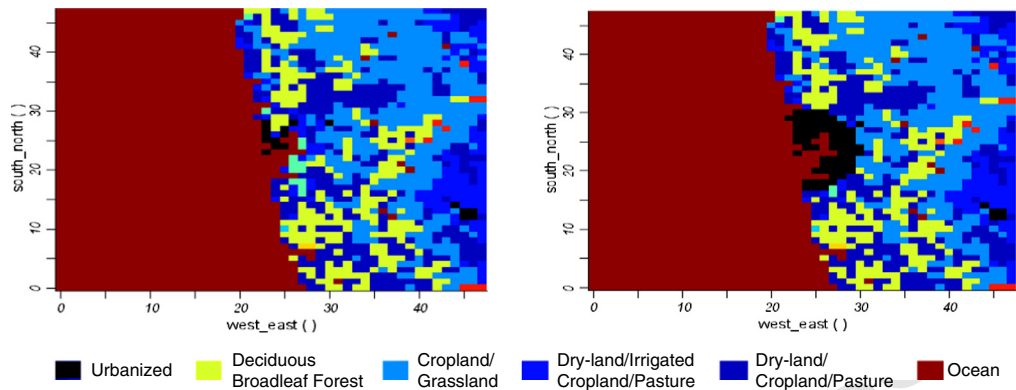


Fig. 4. The landuse transformation introduced in the semi-idealised study for the case of Colombo, Sri Lanka. Left: current, right: transformed.

352 similar to the event documented, as it was difficult to obtain  
 353 suitable rainfall data for all the events for a better validation. As  
 354 an example the accumulated rainfall over the 2007 May rainfall  
 355 event in Colombo is shown in Fig. 6. This event recorded 12 cm  
 356 rainfall at the only meteorological station in the city of Colombo.  
 357 While the model could clearly reproduce the extreme rainfall  
 358 condition around the city, the results are underestimated over  
 359 the city centre. The highest rainfall values are further inland.  
 360 However this discrepancy between point-measurements and  
 361 spatial estimates is quite common due to a number of reasons  
 Q24 like scaling issues (Pathirana et al., 2003, Shem and Shepherd,  
 363 2009). While there are many techniques to improve the  
 364 forecasting outcome of this model, especially in an operational  
 365 setting (e.g. assimilation of local sounding and surface data),  
 366 they are not within the scope of this work.

#### 367 4.3. Results

368 For each city we compared the rainfall output during the  
 369 whole event for the cases of 'Present' and 'Future' scenarios.

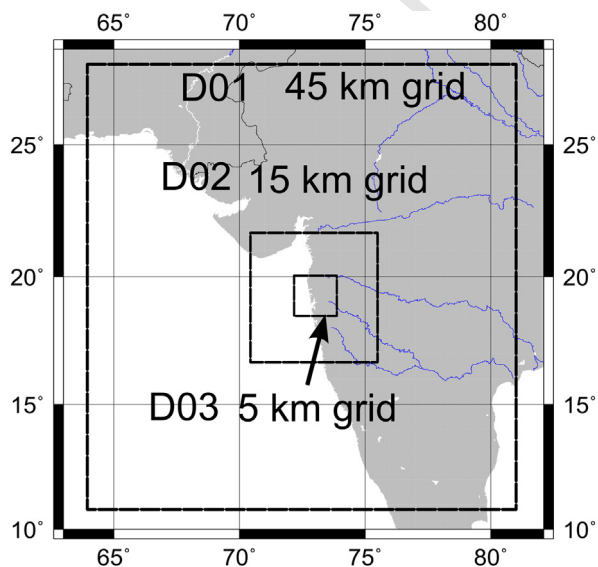


Fig. 5. Nesting scheme used for semi-idealised studies. The case of Mumbai City is shown.

Fig. 7 shows the quantile–quantile plots for each city. These  
 plots were calculated by ordering non-zero grid level rainfall  
 in ascending order and dividing into 100 equal quantiles.  
 Cities of Colombo, Dhaka and Mumbai showed a significant  
 increase of high-intensity rainfalls though the lower-  
 intensities were largely unchanged. However, Taipei did  
 not show any significant change of rainfall due to increased  
 urbanisation.

All cases, including Taipei showed elevation of maximum  
 recorded temperature (daytime) during the simulation period,  
 but the minimum (night-time) temperature remained un-  
 changed. The cases of Dhaka and Taipei are shown in Fig. 8.

#### 5. Urban growth model

The urbanisation scenarios used in the previous semi-  
 idealised case were crude – we simply assumed that the city  
 will grow twice its current diameter and the area will be  
 completely covered with urban landuse. In some cases this  
 might be an approximation of the actual urban growth  
 behaviour; since the 1980s, the city of Beijing, China, ex-  
 perience a tremendous growth which follows an almost  
 perfect radial expansion. Yet, urban growth patterns depend  
 on numerous factors ranging from ground price distribution  
 to physical conditions (e.g. slope and soil conditions). During  
 the last forty years considerable progress has been made in  
 accurately modelling spatially explicit urban development  
 that mimics actual observations over space and time (White  
 and Engelen, 1993; Makse et al., 1995; Ward, 2000; Filho  
 et al., 2009 among many others) and a number of theories  
 like diffusion limited growth (Makse et al., 1995) and  
 cellular-automata (Ward, 2000) has been used as a basis for  
 these models. While initially urban growth was treated like  
 an almost generic phenomenon, currently urban growth  
 models derive transition rules that mimic landuse or land  
 cover changes from historical land use data of actual cities  
 (e.g. Lih and Yeh, 2008; Yang et al., 2008). After an initial  
 training phase in which specific local growth patterns are  
 'learned', prospective growth is determined for future years.  
 Apart from local growth dynamics, top-down information  
 expressing planning constraints (e.g. zoning maps), physical  
 conditions (e.g. variations in slope) and other factors  
 (proximity to infrastructure, economic hotspots, etc.) are  
 used to reflect actual conditions. Depending on the available

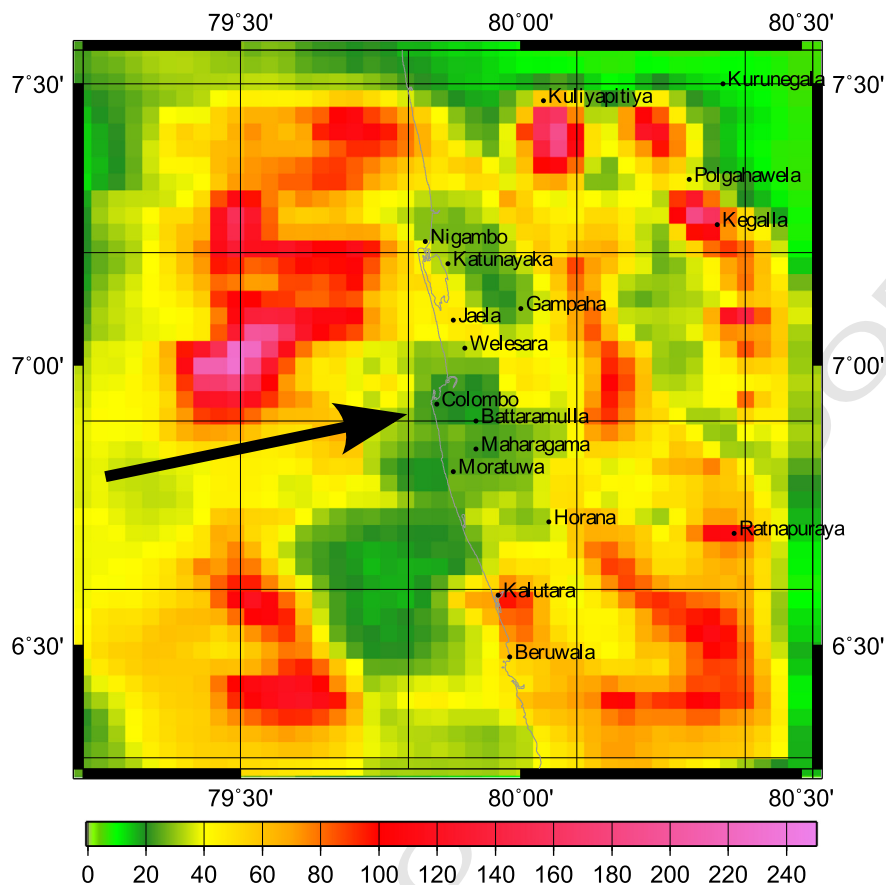


Fig. 6. Accumulated rainfall (mm) from 2 to 3 May 2007 rainfall event simulation. The prevailing surface wind direction is marked by the arrow.

433 data and planning consistency in cities, current urban  
 434 growth models reach a relatively high level of accuracy;  
 435 i.e. retrospective predictions are similar to observed land  
 436 cover or landuse maps.

437 To explore the future urban growth extent for the city of  
 438 Mumbai, we used the urban growth modelling platform  
 439 Dinamica-EGO (Filho et al., 2009) to project the urban  
 440 growth of the city of Mumbai based on its past urban growth  
 441 characteristics. The process of building and validation of the  
 442 urban growth models for Mumbai and several other cities are  
 443 explained by Veerbeek et al. (2011). We used a maximum  
 444 likelihood classification method to derive landuse classi-  
 445 fications for city and surroundings of Mumbai for the base  
 446 years 1992 and 2005 (Fig. 9). Using two significantly apart  
 447 base years (1992 and 2005) the model derived transition  
 448 rules to predict the urban extent for the year 2035 based on a  
 449 'business-as-usual (BAU)' assumption.<sup>1</sup> To derive the proper  
 450 transition rules, additional base maps were used with in-  
 451 formation on infrastructure, morphology (slope, elevation),  
 452 surface water and rivers, etc. Calibration of the model  
 453 resulted in an 85% accuracy on a scale level of  $240 \times 240$  m  
 454 (Veerbeek et al., 2011). Higher levels of accuracy might  
 455 be reached using a more intricate land cover classification

<sup>1</sup> BAU assumption: The transition rules derived from the past apply to the future.

process in combination with additional data on economic 456  
 development, ground price differentiation and planning 457  
 policies. 458

## 6. Mumbai case-study with future urbanisation 459

For the chosen areas, the urban extent of Mumbai and its 460  
 suburbs increases in 2006 by about 22% (to 485 km<sup>2</sup>) 461  
 compared to the base year 1992 (398 km<sup>2</sup>). The growth 462  
 model estimates a less substantial one for the midterm year 463  
 of 2035 (Veerbeek et al., 2011) in which the urban extent 464  
 further increases by about 13% (547 km<sup>2</sup>). Urbanisation 465  
 mainly takes places in the eastern part of Navi Mumbai and 466  
 the northern city of Thane. While currently disjoint, the 467  
 outcomes predict the cities to merge with Mumbai which has 468  
 little possibilities for expansion to the south/west because of 469  
 its location on a peninsula. 470

WRF model routinely uses USGS landuse data, which 471  
 covers the globe at a resolution of about 1 km. Our landuse 472  
 model based data is of a much higher resolution, but has its 473  
 own sources of uncertainties and errors (e.g. classification 474  
 errors). Using USGS data for the 'Present' situation and 475  
 landuse model predictions for 'Future' case does not 476  
 provide a fair basis for investigating the impact of future 477  
 urbanisation due to the very different nature of the two data 478  
 sources. Therefore, we investigated the influence of landuse 479

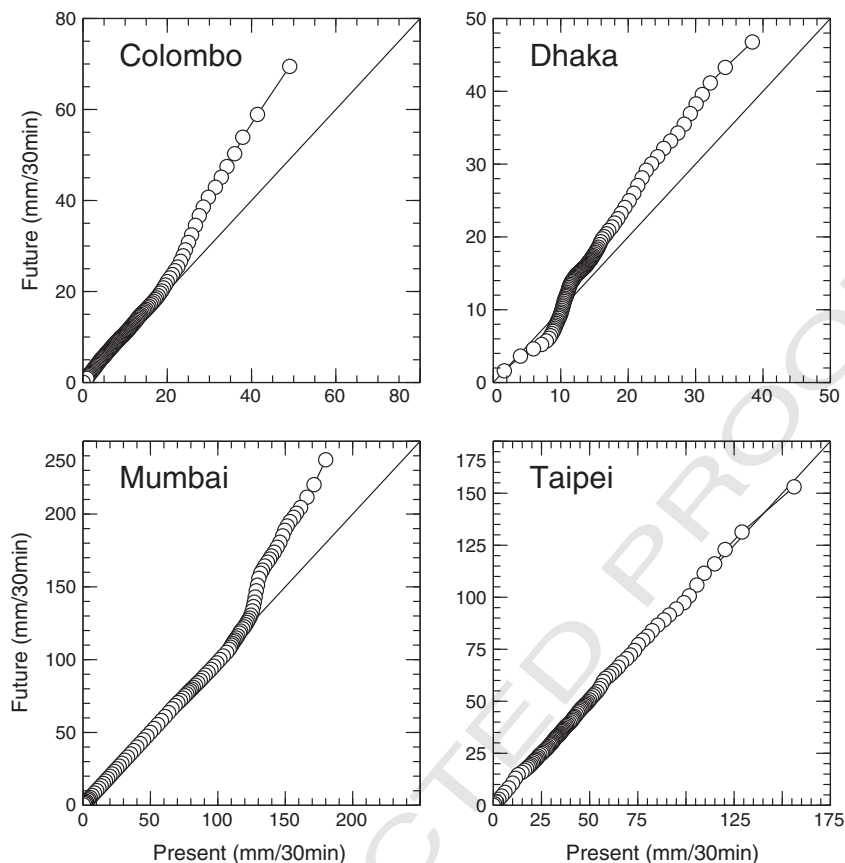


Fig. 7. Quantile–Quantile plots rainfall from model output. The non-zero grid-level rainfall values were sorted and divided into 100 equal quantiles.

480 on extreme rainfall events by using 1992 and 2035 landuse  
481 patterns as follows.

482 As explained in Section 4, the outermost domain of a  
483 mesoscale model has to be fairly large, in-spite of the fact that  
484 the area of interest (covered by innermost grid) is only a few  
485 thousand square kilometres. For this numerical experiment  
486 we constructed three nested domains with resolutions  
487 30 km, 6 km and 1.2 km, covering areas of  $100 \times 100$ ,  
488  $121 \times 121$  and  $46 \times 56$  grids. The urban growth model  
489 covers only a space of approx. 1700 km<sup>2</sup>, which is about half  
490 of the area of the innermost domain. We used the 24  
491 category USGS landuse data to first create the simulation  
492 domain. Then for both ‘Present’ and ‘Future’ scenarios, this  
493 landuse data was patched with the respective model-based  
494 landuse patterns (Fig. 9), and translated into USGS con-  
495 ventions. The procedure of patching is illustrated in Fig. 10.  
496 Then for each grid-cell that was originally non-urban in  
497 USGS data, but urban in the patched data, we decreased the  
498 albedo by 20% and vegetation fraction by 75%. For partially  
499 urbanised cells we reduced the quantities by a percentage  $C$   
500 given by,

$$C = \frac{U_{\text{model}}}{U_{\text{USGS}}} C_0 \quad (1)$$

502 where  $U_{\text{model}}$  and  $U_{\text{USGS}}$  are the urban landuse fraction of the  
503 cell according to patched landuse and original USGS landuse

data, respectively.  $C_0$  is 25% for albedo and 75% for vegetation  
504 fraction. 505

In this simulation we used WRF model with the Noah land  
506 surface model to represent the surface processes. No cumulus  
507 parameterisation was used for the innermost domain as the  
508 grid size of the domain is small enough to fully explicitly  
509 resolve the cumulus formation, by means of cloud micro-  
510 physics. Important model parameters are given in Table 4. 511

The model was integrated for four historical rainstorms  
512 that caused flooding (Table 3), under ‘Present scenario’ and  
513 ‘Future scenario’ conditions. Fig. 11 shows the quantile–  
514 quantile plots for the rainfall simulations for these cases. 515  
516 Quantiles were calculated by sorting grid level rainfall in  
517 descending order and dividing into 100 equal quantiles. 517

Based on the simulation experiments for the four events,  
518 we attempted to analyse the possible change in the extreme  
519 precipitation frequencies. We based our analysis on the  
520 intensity–duration–frequency formula for Western India  
521 proposed by Kothiyari (1992): 522

$$I_t^T = 8.3 \frac{T^{0.2}}{t^{0.71}} (R_{24}^2) \quad (2)$$

where  $I_t^T$  is the intensity of rainfall in mm/h,  $T$  is the return  
523 period in years and  $t$  is the duration in hours.  $R_{24}^2$  is the  
524 magnitude of the two year return period, 24 h duration 526

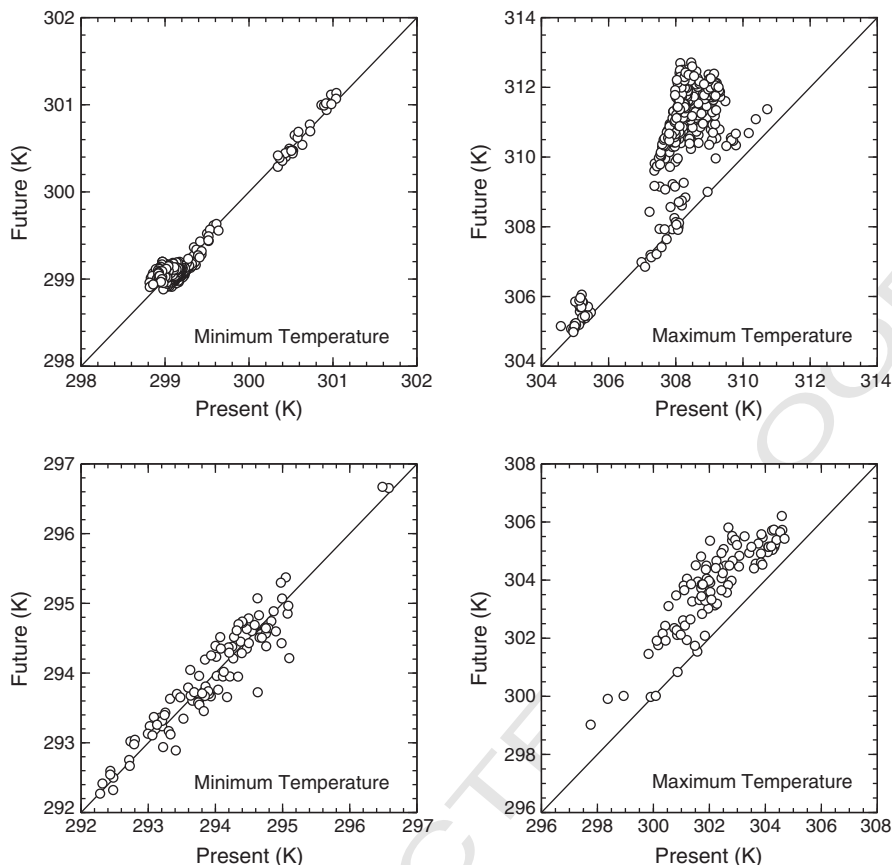


Fig. 8. Simulated maximum (daytime) and minimum (night-time) temperature in Dhaka (top) and Taipei (bottom) during the event.

527 rainfall event volume in mm. Kelkar (2005) estimates the  
 528 two year return period rainfall in Mumbai as 200 mm.  
 529 Instead of 15 min time interval used for reporting the results  
 530 of the rest of the study, we used 1 h as the storm-duration  
 531 for the frequency analysis so that it is possible to compare  
 532 the results of our analysis with commonly measured rainfall.  
 533 We performed a quantile–quantile analysis of all events  
 534 (500 equal quantiles). Then each of the ‘Future’ and ‘Present’  
 535 quantiles was given a return period based on Eq. (2). Fig. 12  
 536 shows the resulting relationship of the return periods.  
 537 According to our findings, the current 10-year rainfall event  
 538 (75 mm/h) would increase its frequency to a 3 year recurrence  
 539 and 50-year (105 mm/h) to 22-year.

## 540 7. Synthesis

541 We performed three sets of numerical experiments in  
 542 order to test the hypothesis that changes in urban landuse  
 543 cause significant changes in extreme rainfall in urban centres  
 544 and surrounding areas. The first experiment was a completely  
 545 idealised one set up within a quasi-2D domain with periodic  
 546 boundary conditions. Keeping all other parameters  
 547 constant, we changed the size of the urban landuse patch  
 548 on the domain. The high rainfall yield over a 60 km area  
 549 starting from the centreline of the city showed a significant  
 550 positive trend with increasing urban landuse. However, the

windward stretch of the city showed a significant reduction  
 551 of high rainfall. This latter phenomenon can easily be explained  
 552 by the use of periodic boundary condition and the limited  
 553 extent of the modelling domain. Due to limited replenishment  
 554 of moisture (small ‘ocean’ area), heavy rainfall in one part of  
 555 the domain would naturally result in the reduction of rainfall in  
 556 another part.  
 557

In real-world cities, the meteorological situation involves  
 558 a number of complexities like impact of topography and  
 559 water bodies, changes in wind direction with time, location  
 560 and elevation and the surface properties are also much more  
 561 heterogeneous. Therefore it is conceivable that the rainfall  
 562 response to urbanisation also should be quite complicated  
 563 in real cities, compared to this idealised study. However, it  
 564 is remarkable that even under these ideal conditions, the  
 565 response of the system to the increased urbanisation was far  
 566 from straight-forward monotonically increasing one. There  
 567 are instances where increasing urbanisation, indeed, caused a  
 568 reduction in high rainfall yield (e.g. urban patch size increase  
 569 from 8 km to 12 km (Fig. 2)). Considering the design of the  
 570 experiment (we repeated each simulation ten times with  
 571 slightly different initial conditions) it is hard to attribute  
 572 this to the complex-system response which is sensitive  
 573 dependent on the initial condition of the system. Seemingly  
 574 this is a real feature of the response of rainfall process to UHI  
 575 growth. Kusaka et al. (2009) discussed a chaotic response of  
 576



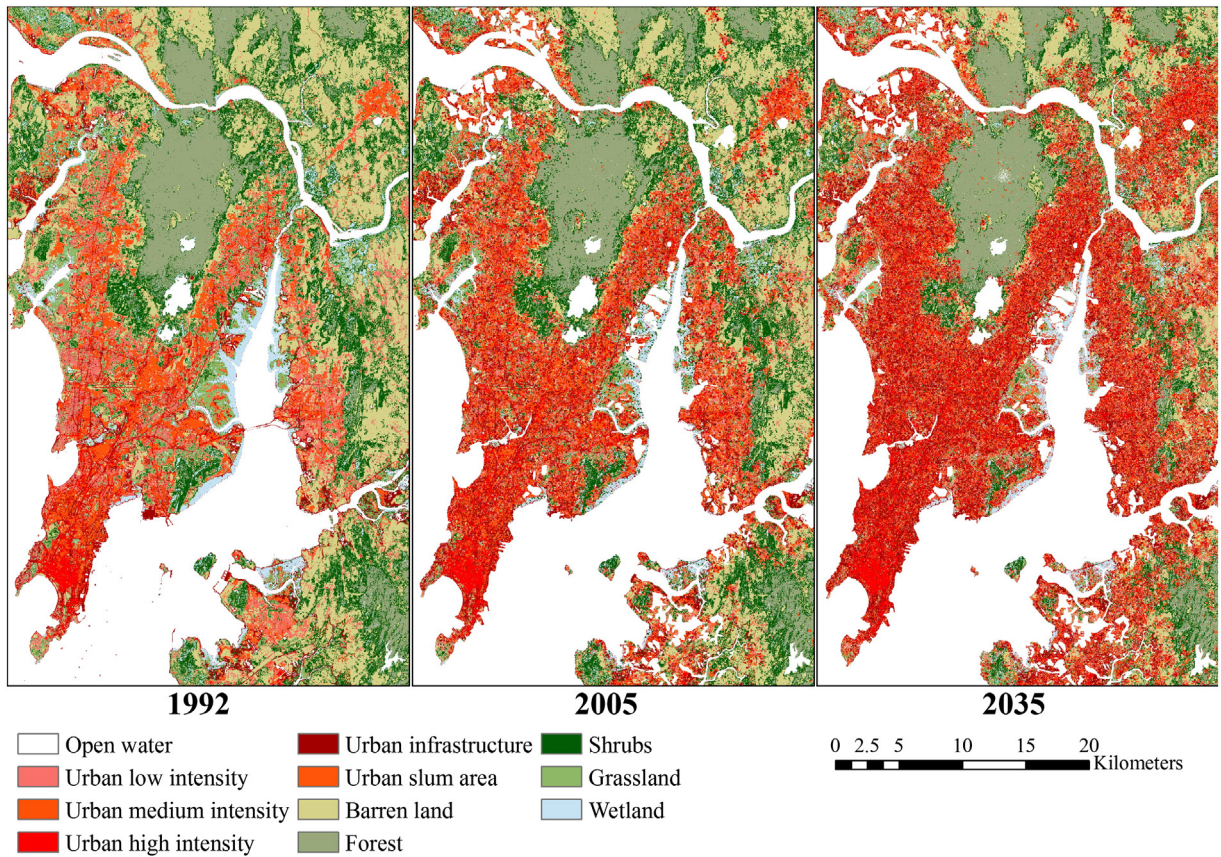


Fig. 9. Landuse classifications derived from LandsAT data (1992, 2005) and Dynamica EGO simulation (2035).

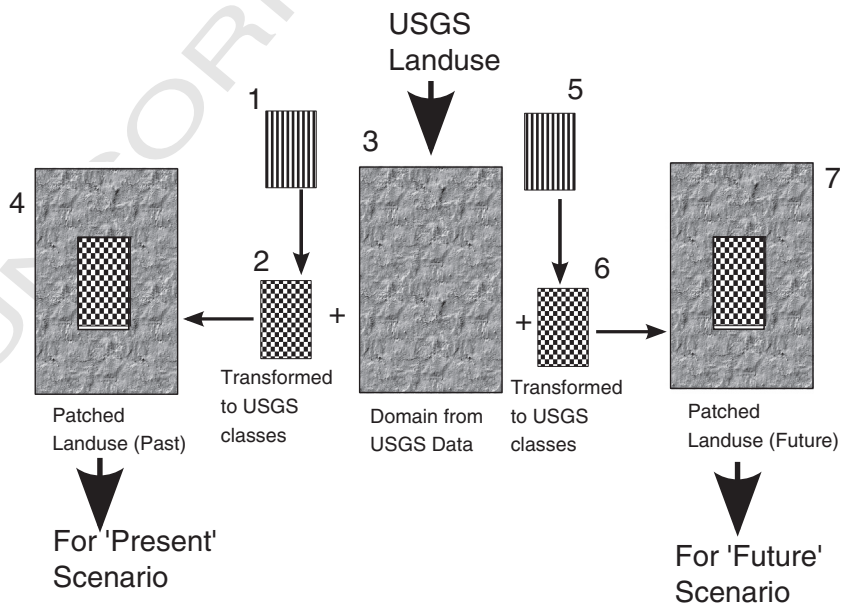


Fig. 10. The landuse patching process. (1) 'Present scenario' landuse map produced by urban growth simulation model, based on its own landuse classes. (2) Same map transformed to USGS 24 category classes. (3) The landuse map created using original USGS landuse data. (4) The patched landuse map used in WRF model simulations for 'Present scenario'. (5),(6),(3) and (7): same procedure for 'Future scenario'.



**Table 3**  
Mumbai rainfall events simulated.

Event	Event date	Simulation	
		Start	End
Event 1 <sup>a</sup>	–	2010-08-22 00:00	2010-08-24 18:00
Event 2	2010-08-30	2010-08-27 00:00	2010-08-30 00:00
Event 3	2007-07-03	2007-07-01 00:00	2007-07-06 18:00
Event 4	2005-07-26	2005-07-24 00:00	2010-08-24 18:00

<sup>a</sup> Event 1 was a large scale event that caused rainfall in many locations in India.

the atmospheric field to landuse change. The non-linear dependence of rainfall activity to the urban size may have resulted from a similar response of the model atmosphere.

One of the signature features of urbanisation is the reduction of the latent heat released by the surface to the upper atmosphere (Fig. 13). The urban landuse typically causes low latent heat release due to the low transpiration as well as low rainfall interception (Nakayoshi et al., 2009) compared to vegetated surfaces. This is one of the major causes of excessive thermal built-up near the surface triggering convective breakup during the daytimes. In these instances the air circulation above the city acts as a virtual mountain, lifting the large-scale wind fields. All simulations in the three sets of experiments showed this behaviour (e.g. Fig. 8). However, the situation is not as straightforward when the UHI causes the rainfall to be enhanced over the city (e.g. Charabi and Bakhit, 2011). The rain increases moisture availability, and could in turn increase the latent heat release by urban landuse. To what extent this would offset the reduction of transpiration depends on a number of factors: The amount of solar radiation (affecting potential evaporation) and the moisture availability (depending on rainfall and surface runoff) are two major ones.

There are many more realistic versions of the radiative transfer. The WRF model has an urban canopy parameterisation scheme that allows for canyon effects of buildings on radiation and winds to be implemented (Salamanca and Martilli, 2010). COAMPS model already uses this in operational simulations (Meir, 2013). In the present studies we did not employ that parameterisation scheme. The impacts of the landuse change is represented in the models only by its influence on the surface scheme – Noah-LSM in first and third cases or thermal diffusion in the second case. While Noah LSM has a simple parameterisation for this impact, these are not specifically detailed for urban environments (Lee et al., 2011). Further studies on explicit parameterisation methods to represent urban land-form accurately are much needed.

**Table 4**  
Important WRF model parameters used in three sets of experiments.

Parameter	Idealised study	Semi-idealised study	Mumbai case
Microphysics	MM5 – Lin et al.		
Short-wave radiation	MM5 – Dudhia scheme		
Long-wave radiation	RRTM scheme		
Surface-layer physics	Noah-LSM with 4 soil layers	MM5 – 5 layer thermal diffusion model	Noah-LSM with 4 soil layers
Boundary layer physics	YSU scheme		
Cumulus parameterisation	None	Betts-Miller-Janjic (outer domains) No cumulus scheme (inner domain)	

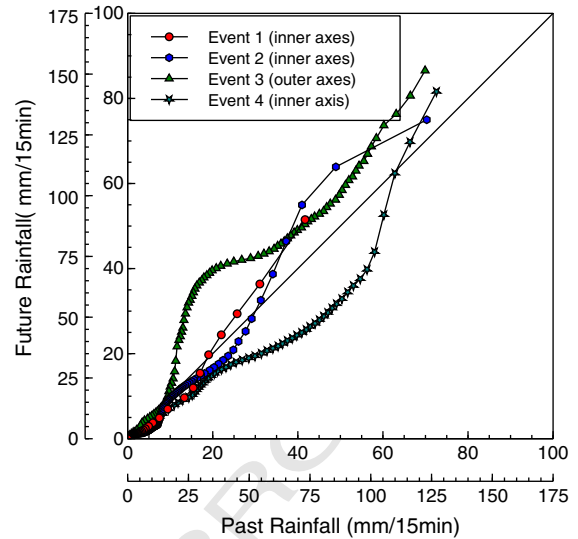
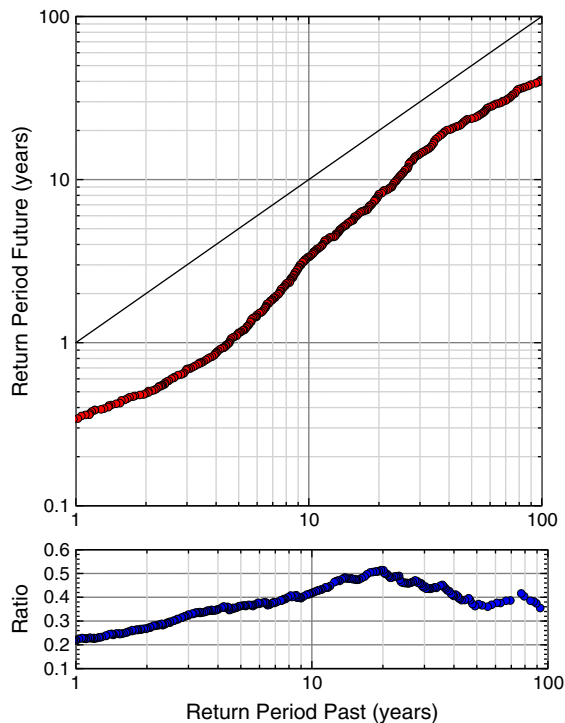


Fig. 11. Quantile–quantile plots of the simulations of four events in Mumbai.

Rainfall frequency analysis based on near-stationary data is a well established technique. Using those techniques for the purpose of demonstrating the changes of extreme values that may result as a change of the climatic system—be it global or regional — is a challenging, if not a seemingly impossible task. The effort towards the result shown in Fig. 12 involves some major assumptions. Extreme value analysis typically needs a long record of (annual) maximum rainfall at a given location, equivalent of which, is hard to obtain in the case of the ‘what-if’ experiments we have conducted. Instead, we sampled a number of model grid points in the general area of the Mumbai City to obtain a varied record of high-intensity rainfall values. The basis for this approach is explained by Pathirana (2011). While this may provide the necessary variability in a statistical sense, the fact remains that all of these values resulted from a few (in our case four) storm events. In a given climate extreme rainfall can be caused by a variety of meteorological situations (e.g. local-convective activity, monsoon, and cyclones) — all of which are impossible to be represented by a limited number of event simulations. For the case of Mumbai this situation is somewhat remedied by the fact that most of the extreme rainfall is caused by summer monsoon events like the ones we simulated. However, for other climates the situation may be much more complex demanding much larger number of simulations.



**Fig. 12.** Top: frequencies of extreme rainfall for current and future scenarios. Bottom: the ratio of (Future Return Period)/(Past Return Period). The frequency of current 10 year magnitude storm would be 3 years and 100 year would be 30 years.

661 The results of urbanisation are markedly different for  
 662 different cities. Cities may grow in quite unplanned fashion  
 663 where much of the vegetation is removed only to be replaced  
 664 by urban sprawl. On the other hand planned urbanisation  
 665 might allow for green spaces that would – among other  
 666 benefits – improve the release of latent heat reduce the  
 667 heat island build-up. The way we have parameterised and

modelled the urban change is simple compared to the 668  
 actual reality. Probably the level of enhancement of rainfall 669  
 due to urban heat island in reality could be somewhat 670  
 overestimated by these experiments. However, we believe 671  
 that the evidence produced is adequate to prove the 672  
 hypothesis that extensive urbanisation can cause changes in 673  
 rainfall in and around cities. Further, we have shown that 674  
 these changes concentrate around extreme rainfall quan- 675  
 tities, compared to small rains. The implications of this 676  
 should be considered in urban planning activities, particu- 677  
 larly in designing new urban drainage infrastructure that 678  
 is expected to last for at least several decades. The more 679  
 accurate quantification of the changes requires further 680  
 research. 681

There are many indications, that the relationship of urban 682  
 heat island caused rainfall enhancement, to the increase of 683  
 urbanisation, while being a significant and positive one, is far 684  
 from simple. For example our idealised experiments showed 685  
 some instances where a certain level of increase in Q32 686  
 urbanisation resulted in a net decrease of rainfall (Fig. 2). 687  
 Our simulation with Taipei did not show any sensitivity of 688  
 rainfall to doubling the city's diameter. A plausible explana- 689  
 tion for this might be the fact that the complex surrounding 690  
 topography involving mountains already play a significant 691  
 role in precipitation formation (Lin et al., 2008), and further 692  
 increase of the urban patch does not contribute to a further 693  
 enhancement of precipitation. 694

In the case of Mumbai the July 2007 storm magnitude 695  
 (Fig. 14) increased over the urban area, but the large 696  
 precipitation on the north of the city was slightly reduced in 697  
 the 'Future' scenario. In a different study Ntelekos et al. (2008) 698  
 have concluded that the severe 2004 July rainstorm over 699  
 Baltimore did not show a sensitivity to UHI. The dynamics of 700  
 the urban heat island formation and the resulting changes in 701  
 the rainfall are complex and depend on a multitude of localised 702  
 parameters like topography, surrounding landuse, and features 703  
 of the local/seasonal climatic regime. In order to make more 704  
 reliable predictions on the impact each locality should be 705  
 studied in detail. It is difficult to generalise the results at the 706

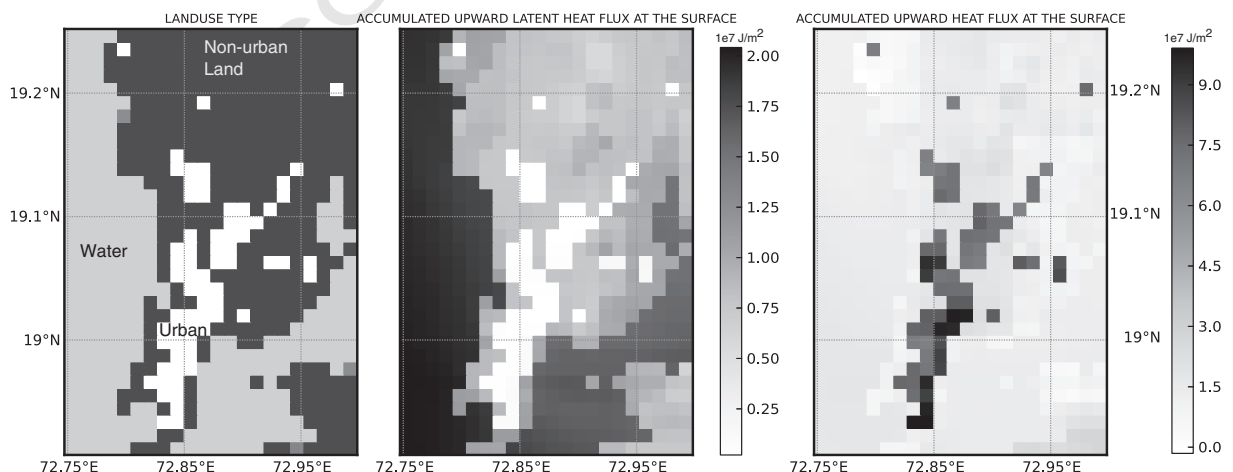


**Fig. 13.** Accumulated latent heat flux (centre) and accumulated total heat flux (right) for 2005 July Mumbai case (Event 4), 'Present scenario'. Corresponding landuse map (simplified) is shown on the left. Urban areas decrease the latent heat flux dramatically, while increasing sensible heat flux (hence the total heat flux is increased).

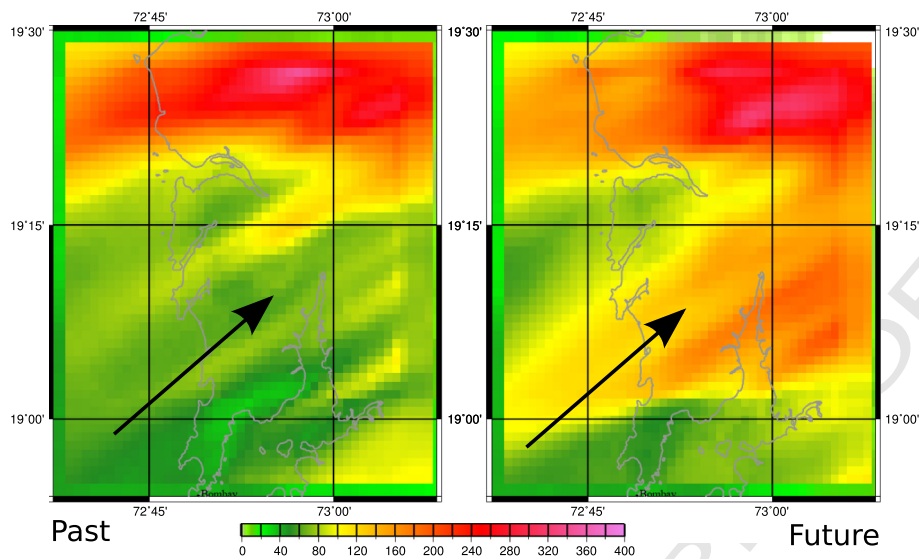


Fig. 14. Total rainfall accumulations (mm) during the 2007 July rainfall event simulation. The prevailing surface wind direction is marked by the arrow.

720 global or even at the regional level. This is an area that deserves  
728 further attention of the climate research community.

### Q33 8. Uncited reference

730 Pathirana and Herath, 1999

### 731 Appendix A. Supplementary data

732 Supplementary data to this article can be found online at  
733 <http://dx.doi.org/10.1016/j.atmosres.2013.10.005>.

### 734 References

- 735 Changnon Jr., S.A., 1979. Rainfall changes in summer caused by St. Louis.  
736 *Science* 205, 402–404.
- 737 Charabi, Yassine, Bakhit, Abdelhamid, 2011. Assessment of the canopy urban  
738 heat island of a coastal arid tropical city: the case of Muscat, Oman.  
739 *Atmos. Res.* 101 (1), 215–227.
- 740 Doyle, J.D., Durran, D.R., 2001. The dynamics of mountain wave induced  
741 rotors. *J. Atmos. Sci.* 59, 186–201.
- 742 Filho, B.S.S., Rodrigues, H.O., Costa, W.L.S., 2009. Modeling Environmental  
743 Dynamics with Dinamica EGO. Instituto de Geociencias-Centro de  
744 Sensoriamento Remoto, Av. Antonio Carlos, Universidade Federal de  
745 Minas Gerais-Campus Pampulha.
- 746 Foley, J.A., DeFries, R., Asner, G.P., Barford, C., Bonan, G., Carpenter, S.R.,  
747 Chapin, F.S., Coe, M.T., Daily, G.C., Gibbs, H.K., Helkowski, J.H., Holloway,  
748 T., Howard, E.A., Kucharik, C.J., Monfreda, C., Patz, J.A., Prentice, I.C.,  
749 Ramankutty, N., Snyder, P.K., 2005. Global consequences of land use.  
750 *Science* 309 (5734), 570–574.
- 751 Jauregui, E., 1996. Urban effects on convective precipitation in Mexico city.  
752 *Atmos. Environ.* 30 (20), 3383–3389.
- 753 Kawabata, T., Seko, H., Saito, K., Kuroda, T., Tamiya, K., Tsuyuki, T., Honda, Y.,  
754 Wakazuki, Y., 2007. An assimilation and forecasting experiment of the  
755 Nerima heavy rainfall with a cloud-resolving nonhydrostatic 4-  
756 dimensional variational data assimilation system. *J. Meteorol. Soc. Jpn.*  
757 85 (3), 255–276.
- 758 Kelkar, R.R., 2005. Understanding the extreme weather events. *Newslett.*  
759 *Indian Water Resour. Soc.* (November).
- 760 Kishtawal, C.M., Niyogi, D., Tewari, M., Pielke, R.A., Shepherd, J.M., 2010.  
761 Urbanization signature in the observed heavy rainfall climatology over  
762 India. *Int. J. Climatol.* 30 (13), 1908–1916.
- 763 Kothiyari, U., 1992. Rainfall intensity duration frequency formula for India.  
764 *J. Hydraul. Eng. ASCE* 118 (2), 323–336.

- Kusaka, H., Kimura, F., Nawata, K., Hanyu, T., Miya, Y., 2009. The chink in the  
765 armor: questioning the reliability of conventional sensitivity experiments  
766 in determining urban effects on precipitation patterns. The 7th  
767 International Conference on Urban Climate, vol. 29 (June).
- Landsberg, H.E., 1981. The urban climate. *International Geophysics*, vol. 28.  
769 Academic Press. 770
- Lee, S.H., Kim, S.W., Angevine, W.M., Bianco, L., McKeen, S.A., Senff, C.J., Trainer, M.,  
771 Tucker, S.C., Zamora, R.J., 2011. Evaluation of urban surface parameterizations  
772 in the WRF model using measurements during the Texas air quality study  
773 2006 field campaign. *Atmos. Chem. Phys.* 11 (5), 2127–2143. 774
- Li, L., 2006. Atmospheric GCM response to an idealized anomaly of  
775 the Mediterranean sea surface temperature. *Clim. Dyn.* 27, 543–552. 776  
<http://dx.doi.org/10.1007/s00382-006-0152-6>. 777
- Lin, C.Y., Chen, W.C., Liu, S.C., Liou, Y.A., Liu, G., Lin, T., 2008. Numerical study  
778 of the impact of urbanization on the precipitation over Taiwan. *Atmos.*  
779 *Environ.* 42 (13), 2934–2947. 780
- Lin, W., Zhang, L., Du, D., Yang, L., Lin, H., Zhang, Y., Li, J., 2009. Quantification  
781 of land use/land cover changes in Pearl River Delta and its impact on  
782 regional climate in summer using numerical modeling. *Reg. Environ.*  
783 *Change* 9 (2), 75–82. 784
- Lowry, W.P., 1998. Urban effects on precipitation amount. *Prog. Phys. Geogr.*  
785 22 (4), 477–520. 786
- Makse, H.A., Havlin, H., Stanley, H.E., 1995. Modelling urban growth. *Nature*  
787 377, 608–612. 788
- Meir, Talmor, Orton, Philip M., Pullen, Julie, Holt, Teddy, Thompson, William  
789 T., Arend, Mark F., 2013. Forecasting the New York City urban heat island  
790 and sea breeze during extreme heat events. *Weather Forecast.* (e-View). **Q39**  
791 Mitchell, K., 2000. The community Noah land-surface model (LSM): users  
792 guide. Technical Report. National Centers for Environmental Prediction  
793 (NCEP), USA. 794
- Nakayoshi, M., Moriwaki, R., Kawai, T., Kanda, M., 2009. Experimental study  
795 on rainfall interception over an outdoor urban-scale model. *Water*  
796 *Resour. Res.* 45, W04415. <http://dx.doi.org/10.1029/2008WR007069>. 797
- NCAR, NCEP, FSL, AFWA, Laboratory, N.R., NOAA, FAA, 2000. *Weather*  
798 *Research and Forecasting Model Website* (Last accessed: Oct 2013). **Q40**  
799 Ntelekos, Alexandros A., Smith, James A., Lynn Baeck, Mary, Krajewski, Witold F.,  
800 Miller, Andrew J., Goska, Radoslaw, 2008. Extreme hydrometeorological  
801 events and the urban environment: dissecting the 7 July 2004 thunderstorm  
802 over the Baltimore MD Metropolitan Region. *Water Resour. Res.* 44 (8).  
803 Pathirana, A., 2011. Pitfalls in using the historical record (or 'stationarity  
804 is dead'). In: Zevenbergen, C., Cashman, A., Evelpidou, N., Pasche, E.,  
805 Garvin, S., Ashley, R. (Eds.), *Urban Flood Management*. CRC Press/  
806 Balkema Taylor & Francis Group, London, pp. 54–59. 807
- Pathirana, A., Herath, S., 1999. Multifactorial modelling and simulation of rain fields  
808 exhibiting spatial heterogeneity. *Hydrol. Earth Syst. Sci.* 6 (4), 695–708. 809
- Pathirana, A., Herath, S., Yamada, T., 2005. Simulating orographic rainfall  
810 with a limited-area, non-hydrostatic atmospheric model under idealized  
811 forcing. *Atmospheric Chemistry and Physics*, 5. European Geosciences  
812 Union 215–226. 813

- 814 Pathirana, A., Herath, S., Yamada, T., Swain, D., 2007. Impacts of anthropogenic  
815 aerosols on south Asian rainfall – a modeling study. *Clim. Change* 85 (1–2),  
816 103–118.
- 817 Royer, Alain, Charbonneau, Lise, Teillet, Philippe M., 1988. Interannual  
818 Landsat-MSS reflectance variation in an urbanized temperate zone.  
819 *Remote Sens. Environ.* 24 (3), 423–446.
- 820 **Q37** Sagan, C., 2000, O.B., Pollack, J.B., 1979. Anthropogenic Albedo changes and  
821 the Earth's climate. *Science* 206 (4425), 1363–1368.
- 822 Salamanca, F., Martilli, A., 2010. A new building energy model coupled with  
823 an urban canopy parameterization for urban climate simulations part II.  
824 Validation with one dimension off-line simulations. *Theor. Appl. Climatol.*  
825 99 (3), 345–356.
- 826 Shem, W., Shepherd, M., 2009. On the impact of urbanization on summertime  
827 thunderstorms in Atlanta: two numerical model case studies. *Atmos. Res.*  
828 92 (2), 172–189.
- 829 Shepherd, J.M., 2005. A review of current investigations of urban-induced  
830 rainfall and recommendations for the future. *Earth Interact.* 9 (12), 1–27.
- 831 Shepherd, J.M., 2006. Evidence of urban-induced precipitation variability in  
832 arid climate regimes. *J. Arid Environ.* 67 (4), 607–628.
- 833 Skamarock, W.C., Klemp, J.B., Dudhia, J., Gill, D.O., Barker, D.M., Wang, W.,  
834 Powers, J.G., 2005. A description of the advanced research WRF version 2.  
835 Technical Report. National Center for Atmospheric Research, Boulder,  
836 Colorado, USA.
- 837 Solomon, S., Qin, D., Manning, M., Chen, Z., Marquis, M., Averyt, K.B., Tignor,  
838 M., Miller, H.L. (Eds.), 2005. *Climate Change 2005 – The Physical Science  
Basis: Working Group I Contribution to the Fourth Assessment Report of  
the IPCC.* Cambridge University Press, Cambridge, UK and New York, NY,  
USA. 839–841
- 842 Subbiah, S., Vishwanath, V., Kaveri Devi, S., 1990. Urban climate in Tamil Nadu,  
843 India: a statistical analysis of increasing urbanization and changing trends  
844 of temperature and rainfall. *Energy Build.* 15 (1–2), 231–243.
- 845 Taha, H., Akbari, H., Rosenfeld, A., Huang, J., 1988. Residential cooling loads  
846 and the urban heat island – the effects of albedo. *Build. Environ.* 23 (4),  
847 271–283.
- 848 Takahashi, H., 2003. Secular variation in the occurrence property of summertime  
849 daily rainfall amount in and around the Tokyo Metropolitan area. *Tenki* 49,  
850 31–41 (In Japanese, with abstract in English).
- 851 Veerbeek, W., Deneke, H.B., Pathirana, A., Bacchin, T., Brdjanovic, D., 2011.  
852 Urban growth modeling to predict the changes in the urban  
853 microclimate and urban water cycle. 12th International Conference on  
854 Urban Drainage Modelling, Brazil.
- 855 Ward, D., 2000. A stochastically constrained cellular model of urban growth.  
856 *Comput. Environ. Urban Syst.* 24 (6), 539–558.
- 857 Watkins, Richard, Kolokotroni, Maria, 2013. The London Urban Heat Island –  
858 Upwind Vegetation Effects on Local Temperatures. PLEA2012 – 28th  
859 Conference, Opportunities, Limits & Needs Towards An Environmentally  
860 Responsible Architecture; Lima, Perú 7–9 November 2012.
- 861 White, R., Engelen, G., 1993. Cellular automata and fractal urban form: a  
862 cellular modelling approach to the evolution of urban land-use patterns.  
863 *Environ. Plan. A* 25 (8), 1175–1199.
- 864